

Was the February 2022 Persistent Heavy Precipitation Event over South China Enhanced by Anthropogenic Climate Change?

Shaobo Qiao, Dong Chen, Meng He, Chao Li, Chundi Hu, Junhu Zhao, Jianbo Cheng, and Guolin Feng

AFFILIATIONS: Qiao—School of Atmospheric Sciences, Sun Yat-sen University, and Southern Marine Science and Engineering Guangdong Laboratory (Zhuhai), and Key Laboratory of Tropical Atmosphere–Ocean System, Ministry of Education, Sun Yat-sen University, Zhuhai, China; Chen and He—School of Atmospheric Sciences, Sun Yat-sen University, and Southern Marine Science and Engineering Guangdong Laboratory (Zhuhai), Zhuhai, China; Li—Key Laboratory of Geographic Information Science, Ministry of Education, and School of Geographic Sciences, East China Normal University, Shanghai, China; Hu—Ocean College, Zhejiang University, Hangzhou, China; Zhao—Laboratory for Climate Studies, National Climate Center, China Meteorological Administration, Beijing, China; Cheng—School of Environmental Science and Engineering, Yancheng Institute of Technology, Yancheng, China; Feng—School of Physical Science and Technology, Yangzhou University, Yangzhou, and Laboratory for Climate Studies, National Climate Center, China Meteorological Administration, Beijing, China

<https://doi.org/10.1175/BAMS-D-22-0258.1>

CORRESPONDING AUTHOR: Chao Li, cli@geo.ecnu.edu.cn

Supplemental material: <https://doi.org/10.1175/BAMS-D-22-0258.2>

In final form 16 October 2023

© 2023 American Meteorological Society. This published article is licensed under the terms of the default AMS reuse license. For information regarding reuse of this content and general copyright information, consult the AMS Copyright Policy (www.ametsoc.org/PUBSReuseLicenses).

Annual maximum 7-day precipitation has increased over South China since 1961. Ten CMIP6 climate models simulate either weaker increases in risk ratio than observed or nonsignificant changes.

During 17–23 February 2022, an exceptionally persistent heavy precipitation event occurred in South China (18°–30°N, 107°–122°E; the mainland region marked by magenta rectangle in Fig. 1a), with the regional mean 7-day precipitation accumulation exceeding the 1961–2020 climatology by three standard deviations. The event and the accompanying extremely low temperatures and sharply decreased sunshine have exerted damaging impacts on local crop production, transportation, and power supply according to the China Climate Bulletin in 2022 (www.cma.gov.cn/2011xwzx/2011xmtjj/202302/t20230207_5293467.html).

In addition to the effects of natural variability such as El Niño–Southern Oscillation (Zhang et al. 1996; Wang et al. 2000), the Pacific decadal oscillation (Wang et al. 2008; Kim et al. 2014), and the Madden–Julian oscillation (Jeong et al. 2005; Wen et al. 2009; Park et al. 2010; He et al. 2011), anthropogenic climate change tends to also affect winter extreme precipitation in South China (Hu et al. 2021; He et al. 2021). Using the wintertime (December–February) maximum of regional mean precipitation accumulations over 1 week (hereafter as Rx7day) as a measure of the severity of persistent heavy precipitation event, here we attempt to seek observational and climate model evidence of the influence of the ongoing anthropogenic global warming on this heavy precipitation event.

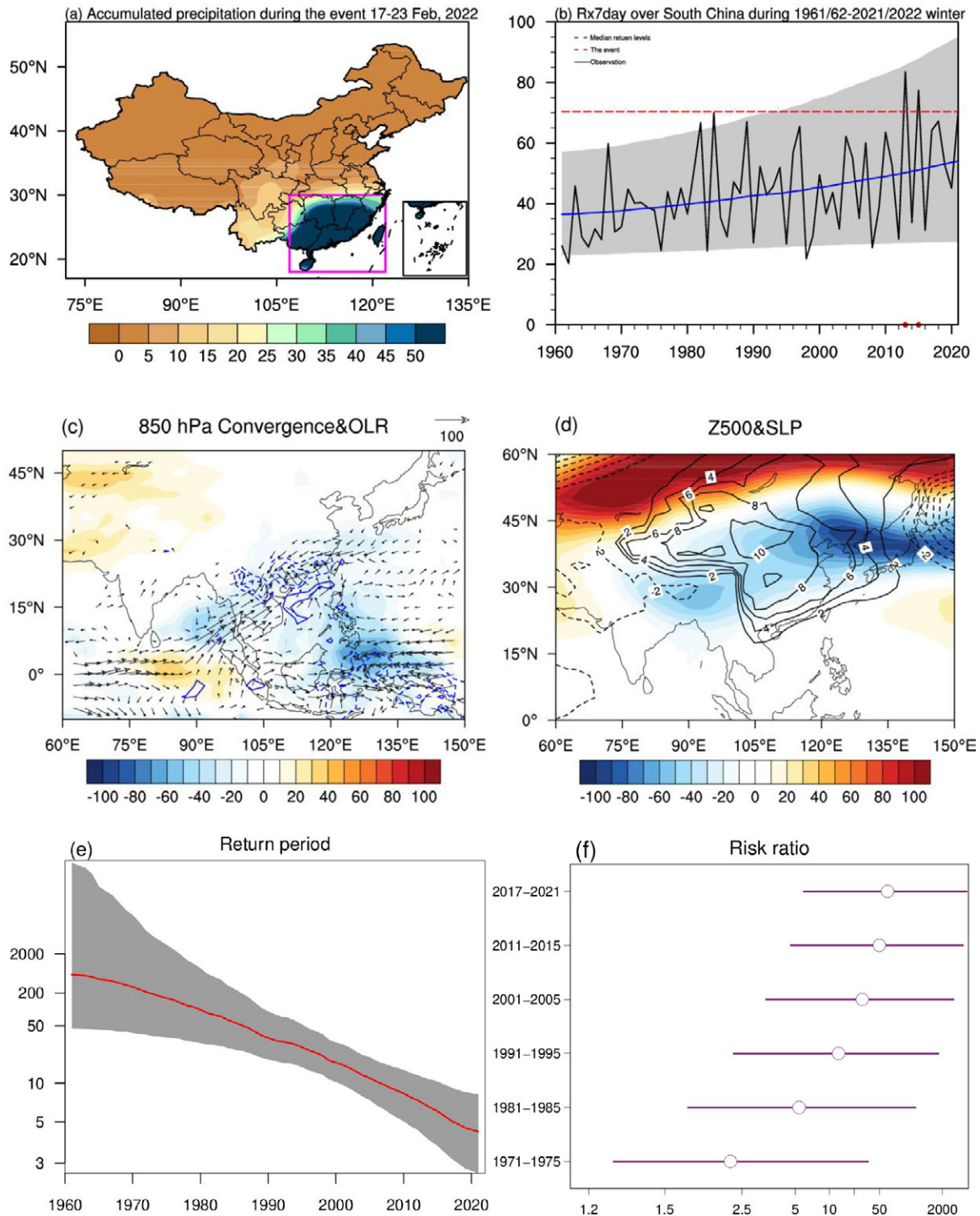


Fig. 1. (a) Observed accumulated precipitation (shading; mm) during the event on 17–23 Feb 2022. (b) Time series of Rx7day (black line) during 1961/62–2022/22 winters averaged over South China [18°–30°N, 107°–122°E; magenta rectangle in (a)] and the median (blue line) and 5th and 95th quantiles (gray shading) of the estimated nonstationary GEV distribution. (c) Map of outgoing longwave radiation (shaded; $W m^{-2}$), 850-hPa moisture flux anomalies (arrows; $10^{-1} g m^{-1} s^{-1} Pa^{-1}$) and convergence (contour interval: $4 \times 10^{-6} g m^{-2} s^{-1} Pa^{-1}$; the zero contours are omitted) during the event on 17–23 Feb 2022. (d) As in (c), but for 500-hPa geopotential height anomalies (shading; gpm) and sea level pressure anomalies (contours with an interval of 2 hPa; zero contours are omitted). (e) The evolution of return periods and their 5%–95% confidence intervals during 1961/62–2022/22 winters for the observed extreme precipitation event in February 2022. (f) Median risk ratios and their 5%–95% confidence intervals comparing the probability of the observed event during 5-yr moving windows since 1971/72–1975/76 winters relative to the fixed reference period of 1961/62–1965/66.

Data and methods

Daily precipitation observations from 547 weather stations over South China for the 1961/62–2021/22 winters acquired from the National Meteorological Information Center in China are used to compute regional mean Rx7day (the magenta rectangle region marked in Fig. 1; see Fig. S1a in the online supporting information for the locations of the 547 stations; <https://doi.org/10.1175/BAMS-D-22-0258.2>) for each winter. To reflect the effect of human-induced global warming on Rx7day since 1961, we model the time series of regional mean Rx7day for winters of 1961/62–2021/22 via a generalized extreme value (GEV) distribution with varying parameters with total atmospheric CO₂ concentrations, which are chosen to emulate the effects of secular global warming (Risser and Wehner 2017). The annual mean global atmospheric CO₂ concentrations are provided by the Global Monitoring Laboratory (www.esrl.noaa.gov/gmd/ccgg/trends/global.html; Ballantyne et al. 2012). Based on the likelihood ratio test at a significance level of 5% (Table S1), we find that a GEV distribution with both location and scale parameters varying with atmospheric CO₂ concentrations fits the observed regional mean Rx7day time series better than those with constant parameters or varying location or scale parameter only (Table S1). Also, we verified that further increasing the complexity of the GEV distribution did not notably improve the goodness of model–data fit.

We also conduct the same analyses using simulations of regional mean Rx7day from 10 climate models participating in the Coupled Model Intercomparison Project phase 6 (CMIP6; see Table S2 for the detailed information of the used climate models; Eyring et al. 2016), which provide 3 or more merged historical simulations up to 2014 and the shared socioeconomic pathway (SSP) 2–4.5 simulations representing the medium emissions and warming afterward (O’Neill et al. 2016). Daily precipitation observations and simulations are interpolated to the same spatial resolution of 1.0° × 1.0° through area-weighted averaging prior to analysis. To alleviate the influence of model bias in the magnitudes of precipitation extremes, for each model, we identify a model event that is as extreme in occurrence probability as the observed event in the observation time series. To be specific, the model event is chosen such that it has the same exceedance probability or return period in climate model simulations as in the observations during the recent past winters of 2017/18–2021/22 according to the estimated nonstationary GEV distributions for observations and simulations, respectively (Fig. S1b). As for the observations, we select the best GEV distribution for each climate model by the likelihood ratio test at a significance level of 5%. It is noted that the best GEV distribution varies among climate models and can differ from the best one for the observations. For both observations and simulations, we use risk ratio or equivalently changes in return period to quantify the extent to which anthropogenic disturbance of Earth’s climate (as represented by the historical increases of atmospheric CO₂ concentrations) has altered the likelihood of such a persistent heavy precipitation event as observed during 17–23 February 2022 (e.g., Stott et al. 2004). The risk ratio is estimated by comparing the frequency of 7-day events as severe as the observed one in the recent past 2017/18–2021/22 winters with that during the earlier 1961/62–1965/66 winters with relatively weak anthropogenic influence. Uncertainty of the estimated return periods and risk ratios are inferred in terms of a commonly used parametric bootstrap procedure for nonstationary GEV distribution (e.g., Heffernan and Tawn 2004; Hanel et al. 2009; Li et al. 2019).

Results

More frequent 7-day precipitation event. The average of daily precipitation accumulations during 17–23 February 2022 over the 547 stations in South China was above 70 mm, which is the largest Rx7day precipitation accumulation in the 2021/22 winter (Fig. 1a). Based on the latest European Centre for Medium-Range Weather Forecasts reanalysis (ERA5; Hersbach

and Dee 2016), this extreme precipitation event was associated with the convergence of the anomalous moist and warm airflow from the tropical Indo-Pacific Ocean and the northeasterly cold airflow anomalies over South China (Fig. 1c), while the accompanying cold spells tended to be associated with a deepened East Asian trough and a stronger Siberian high (Fig. 1d). It is found that 7-day precipitation events as severe or severer than this observed one occurred three times during the last decade (in the winters of 2013/14, 2015/16, and 2021/22), but such events did not occur before the recent decade (Fig. 1b). Also, the observed Rx7day time series exhibited an overall upward tendency with growing year-to-year variability. These results indicate more frequent extreme 7-day precipitation events against the background of the ongoing global warming, as will be confirmed later.

Observed Rx7day change as a function of global atmospheric CO₂ concentrations. By modeling the observed Rx7day time series via a GEV distribution with nonstationary location and scale parameters varying with atmospheric CO₂ concentrations, there appeared increasing median values in the observed 7-day precipitation accumulations (blue line in Fig. 1b), suggesting that 7-day heavy precipitation events have become more extreme since 1961. The 5th–95th-percentile range of the estimated GEV distribution covers about 90% of the observations (gray shading in Fig. 1b), indicating that the estimated nonstationary GEV distribution provides a reasonable fit to the observed Rx7day time series. It is noted again that the GEV distribution with varying location and scale parameters provides a significantly better fit to the observations than a stationary distribution, while more complex distributions do not substantially improve the quality of fit, according to a likelihood ratio test at the 5% significance level (Table S1).

Based on the estimated GEV distribution, we then estimated the return periods for extreme events with 7-day precipitation accumulations comparable to or larger than the observed value of the February 2022 event for moving 5-yr windows during 1961/62–2021/22 winters using the corresponding 5-yr means of atmospheric CO₂ concentrations, as shown in Fig. 1e for the estimated average return periods as represented for middle years of the moving windows. We observed a substantial decrease in the return period estimates from about 532 years (46 to >10,000 years for the 5%–95% uncertainty range) during the first 5-yr window (i.e., 1961/62–1965/66 winters) to about 4 years (3–8 years) during the last 5-yr window (2017/18–2021/22; Fig. 1e). Correspondingly, the risk ratio estimates for the 5-yr moving windows during 1961/62–2021/22 relative to the 1961/62–1965/66 reference period show a dramatic increase (Fig. 1f). In particular, the risk ratio for the event in 2017/18–2021/22 relative to 1961/62–1965/66 is about 70 (5.7 to >10,000; Fig. 1f). The above results suggest that the likelihood of 7-day extreme precipitation events as the observed one has increased in South China as the global atmospheric CO₂ accumulates.

Simulated Rx7day change with atmospheric CO₂ concentrations. Similarly, the corresponding risk ratios have also been estimated based on climate model simulations, as shown in Fig. 2a for each of the considered climate models. In contrast to the increasing risk ratio in the observations, the risk ratios between the winters during 2017/18–2021/22 and 1961/62–1965/66 are not significantly different from one in 8 of 10 climate models (Fig. 2a), suggesting that these models do not simulate increases in the likelihood of extreme precipitation events as the observed one. The two exceptions are the models of MIROC6 and CanESM5, which produce risk ratios being significantly larger than one, but substantially smaller than the observed value (Fig. 2a).

The lack of a detectable increasing tendency in the simulated Rx7day in these climate models is also consistent with the results derived from a fingerprinting method designed

particularly for climate extremes (Fig. S2), which regresses the observed Rx7day time series to the corresponding modeled responses in a GEV framework (e.g., Zwiers et al. 2011; Liu et al. 2022). In addition to the large internal climate variability of precipitation extremes in a relatively small region as studied here, the lack of detectable tendency of Rx7day increase in the simulations can be also due to the limited skill of the considered climate models in simulating precipitation extremes in South China and their responses to global warming (Fig. S3). Different models exhibit divergent skills in simulating Rx7day in South China (Fig. S1; e.g., Philip et al. 2020). Nevertheless, we confirmed that models with relatively better skill in simulating the 1961/62–2021/22 winter Rx7day climatology (Fig. S1d) and the cycle of seasonal

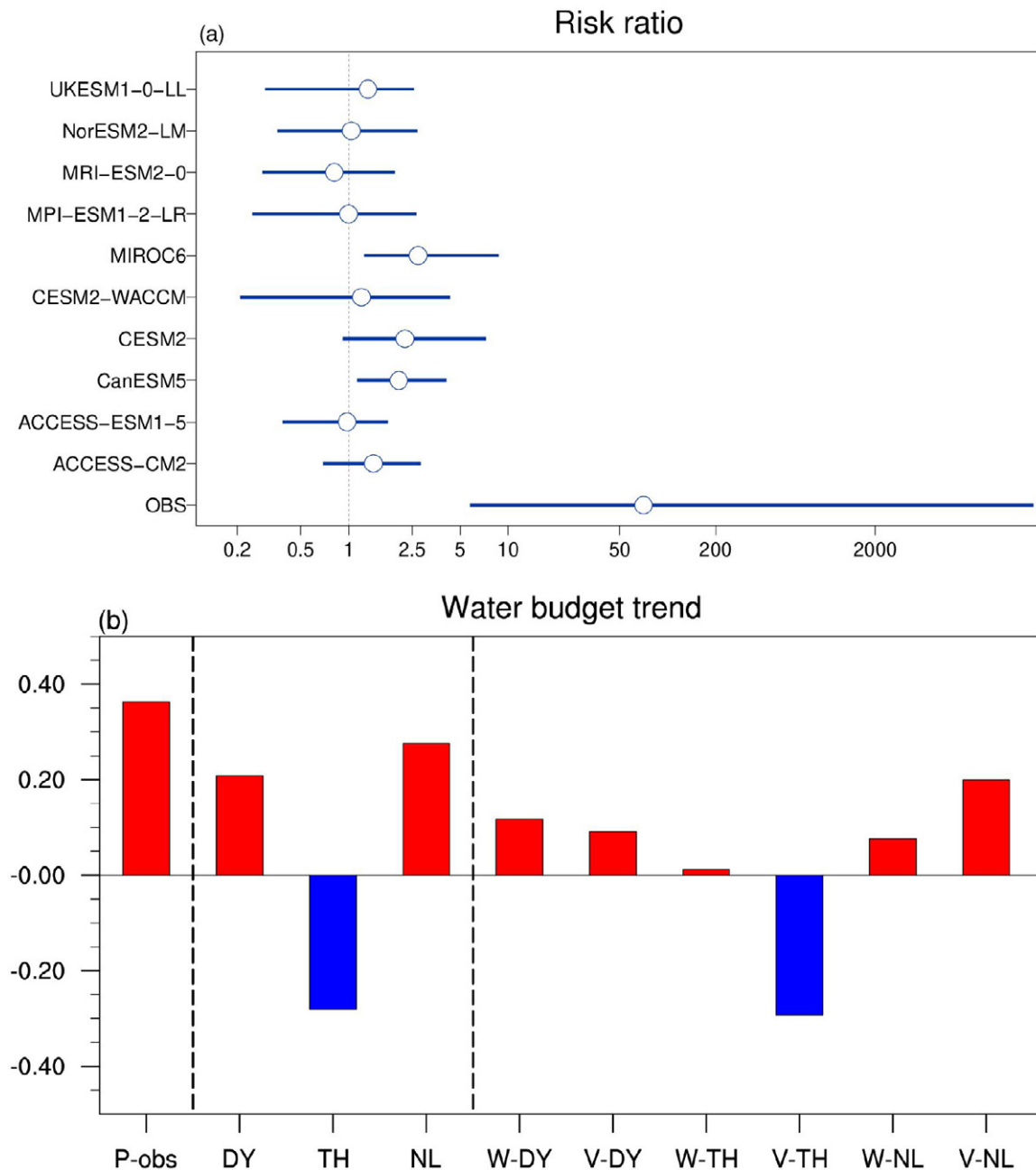


Fig. 2. (a) Median risk ratios and their 5%–95% confidence intervals comparing the estimated probability of the observed event during the 2017/18–2022/22 winters relative to 1961/62–1965/66 winters inferred from observations and climate model simulations. (b) Observed linear trends of winter Rx7day (mm yr⁻¹) and the associated moisture budget terms (10⁻⁶ kg m⁻² s⁻¹ yr⁻¹) averaged over South China during 1961/62–2022/22 (see details of the budget terms in supporting online information).

precipitation accumulations (e.g., ACCESS-CM2 and UKESM1-0-LL; Fig. S1c) did not show discernable advantages in reproducing the observed risk ratio (Fig. 2a).

Conclusions and discussion

Our observational analysis reveals a significant increase in the likelihood of persistent heavy precipitation events in South China as the one occurred in February 2022 since 1961 as a function of global atmospheric CO₂ concentrations, whereas the climate model simulations present no discernable or weaker changes than observed. The underestimation of observed increases in Rx7day by these climate models are probably due to model biases and/or uncertainty from internal climate variability (e.g., Li and Otto 2022). This indicates that the lack of anthropogenic global warming fingerprints in the simulated extreme precipitation events can be uncertain at regional scales, and thus, the design of adaptation policies for regional precipitation extremes such as in South China should not ignore the observational evidence for the possible intensification of extreme precipitation in response to the ongoing global warming.

By an atmospheric moisture budget analysis (Trenberth and Fasullo 2013; see more details in online supporting information), we find that the increasing trends in the observed Rx7day in South China are primarily contributed by changes in factors associated with atmospheric circulations conducive to precipitation extremes (the red bar marked by DY in Fig. 2b), while changes in atmospheric moisture have played a role in weakening 7-day extreme precipitation events (the blue bar marked by TH in Fig. 2b). The dynamic intensification of Rx7day events over South China is associated with anomalous low-level anticyclones over the Philippine Sea (Fig. S4a), which may be partly resulted from the warming over the warm pool in Indo-Pacific Ocean due likely to anthropogenic influence (Funk and Hoell 2015). The thermodynamic decrease in Rx7day is dominated by the horizontal advection of moisture over South China (the blue bar marked by V-TH in Fig. 2b), which is associated with the enhanced east–west gradient of moisture resulting from heterogeneous increase of moisture (Fig. S4b). The combined effects of the enhanced south–north gradient of moisture and low-level southwesterly winds anomalies over South China contribute to the increase of the nonlinear term (Fig. S4c and red bar marked by NL in Fig. 2b). The moisture budget analysis suggests that, to improve the simulation of changes in wintertime precipitation extremes in South China, more attention should be paid to improving the simulation of heterogeneous increase of sea surface temperature and moisture in response to global warming.

Acknowledgments. We acknowledge the support of the Key Program of the National Natural Science Foundation of China (42130610), the General Program of the National Natural Science Foundation of China (42175028, 42075026), Key Laboratory of South China Sea Meteorological Disaster Prevention and Mitigation of Hainan Province (SCSF202201), and the Innovation Group Project of Southern Marine Science and Engineering Guangdong Laboratory (Zhuhai) (311022006).

References

- Ballantyne, A. P., C. B. Alden, J. B. Miller, P. P. Tans, and J. W. C. White, 2012: Increase in observed net carbon dioxide uptake by land and oceans during the last 50 years. *Nature*, **488**, 70–72, <https://doi.org/10.1038/nature11299>.
- Eyring, V., S. Bony, G. A. Meehl, C. A. Senior, B. Stevens, R. J. Stouffer, and K. E. Taylor, 2016: Overview of the Coupled Model Intercomparison Project phase 6 (CMIP6) experimental design and organization. *Geosci. Model Dev.*, **9**, 1937–1958, <https://doi.org/10.5194/gmd-9-1937-2016>.
- Funk, C. C., and A. Hoell, 2015: The leading mode of observed and CMIP5 ENSO-residual sea surface temperatures and associated changes in Indo-Pacific climate. *J. Climate*, **28**, 4309–4329, <https://doi.org/10.1175/JCLI-D-14-00334.1>.
- Hanel, M., T. A. Buishand, and C. A. T. Ferro, 2009: A nonstationary index flood model for precipitation extremes in transient regional climate model simulations. *J. Geophys. Res.*, **114**, D15107, <https://doi.org/10.1029/2009JD011712>.
- He, J., H. Lin, and Z. Wu, 2011: Another look at influences of the Madden-Julian oscillation on the wintertime East Asian weather. *J. Geophys. Res.*, **116**, D03109, <https://doi.org/10.1029/2010JD014787>.
- He, Y., K. Wang, and D. Qi, 2021: Roles of anthropogenic forcing and natural variability in the record breaking low sunshine event in January–February 2019 over the middle-lower Yangtze Plain [in “Explaining Extreme Events of 2019 from a Climate Perspective”]. *Bull. Amer. Meteor. Soc.*, **102** (1), S75–S81, <https://doi.org/10.1175/BAMS-D-20-0185.1>.
- Heffernan, J. E., and J. A. Tawn, 2004: A conditional approach for multivariate extreme values (with discussion). *J. Roy. Stat. Soc.*, **66B**, 497–546, <https://doi.org/10.1111/j.1467-9868.2004.02050.x>.
- Hersbach, H., and D. Dee, 2016: ERA5 reanalysis is in production. *ECMWF Newsletter*, No. 147, ECMWF, Reading, United Kingdom, 7, www.ecmwf.int/en/newsletter/147/news/era5-reanalysis-production.
- Hu, Z., and Coauthors, 2021: Was the extended rainy winter 2018/19 over the middle and lower reaches of the Yangtze River driven by anthropogenic forcing [in “Explaining Extreme Events of 2019 from a Climate Perspective”]? *Bull. Amer. Meteor. Soc.*, **102** (1), S67–S73, <https://doi.org/10.1175/BAMS-D-20-0127.1>.
- Jeong, J. H., C. H. Ho, B. M. Kim, and W. T. Kwon, 2005: Influence of the Madden-Julian oscillation on wintertime surface air temperature and cold surges in East Asia. *J. Geophys. Res.*, **110**, D11104, <https://doi.org/10.1029/2004JD005408>.
- Kim, J. W., S. W. Yeh, and E. C. Chang, 2014: Combined effect of El Niño–Southern Oscillation and Pacific decadal oscillation on the East Asian winter monsoon. *Climate Dyn.*, **42**, 957–971, <https://doi.org/10.1007/s00382-013-1730-z>.
- Li, C., F. Zwiers, X. Zhang, and G. Li, 2019: How much information is required to well constrain local estimates of future precipitation extremes? *Earth’s Future*, **7**, 11–24, <https://doi.org/10.1029/2018EF001001>.
- Li, S., and F. Otto, 2022: The role of human-induced climate change in heavy rainfall events such as the one associated with Typhoon Hagibis. *Climatic Change*, **172**, 7, <https://doi.org/10.1007/s10584-022-03344-9>.
- Liu, Y., C. Li, Y. Sun, F. Zwiers, X. Zhang, Z. Jiang, and F. Zheng, 2022: The January 2021 cold air outbreak over eastern China: Is there a human fingerprint [in “Explaining Extreme Events of 2020 from a Climate Perspective”]? *Bull. Amer. Meteor. Soc.*, **103** (3), S50–S54, <https://doi.org/10.1175/BAMS-D-21-0143.1>.
- O’Neill, B. C., and Coauthors, 2016: The Scenario Model Intercomparison Project (ScenarioMIP) for CMIP6. *Geosci. Model Dev.*, **9**, 3461–3482, <https://doi.org/10.5194/gmd-9-3461-2016>.
- Park, T. W., C. H. Ho, S. Yang, and J. H. Jeong, 2010: Influences of Arctic oscillation and Madden-Julian oscillation on cold surges and heavy snowfalls over Korea: A case study for the winter of 2009–2010. *J. Geophys. Res.*, **115**, D23122, <https://doi.org/10.1029/2010JD014794>.
- Philip, S., and Coauthors, 2020: A protocol for probabilistic extreme event attribution analyses. *Adv. Stat. Climatol. Meteor. Oceanogr.*, **6**, 177–203, <https://doi.org/10.5194/ascmo-6-177-2020>.
- Risser, M. D., and M. F. Wehner, 2017: Attributable human-induced changes in the likelihood and magnitude of the observed extreme precipitation during Hurricane Harvey. *Geophys. Res. Lett.*, **44**, 12 457–12 464, <https://doi.org/10.1002/2017GL075888>.
- Stott, P. A., D. A. Stone, and M. R. Allen, 2004: Human contribution to the European heatwave of 2003. *Nature*, **432**, 610–614, <https://doi.org/10.1038/nature03089>.
- Trenberth, K. E., and J. T. Fasullo, 2013: Regional energy and water cycles: Transports from ocean to land. *J. Climate*, **26**, 7837–7851, <https://doi.org/10.1175/JCLI-D-13-00008.1>.
- Wang, B., R. Wu, and X. Fu, 2000: Pacific–East Asian teleconnection: How does ENSO affect East Asian climate? *J. Climate*, **13**, 1517–1536, [https://doi.org/10.1175/1520-0442\(2000\)013<1517:PEATHD>2.0.CO;2](https://doi.org/10.1175/1520-0442(2000)013<1517:PEATHD>2.0.CO;2).
- Wang, L., W. Chen, and R. Huang, 2008: Interdecadal modulation of PDO on the impact of ENSO on the East Asian winter monsoon. *Geophys. Res. Lett.*, **35**, L20702, <https://doi.org/10.1029/2008GL035287>.
- Wen, M., S. Yang, A. Kumar, and P. Zhang, 2009: An analysis of the large-scale climate anomalies associated with the snowstorms affecting China in January 2008. *Mon. Wea. Rev.*, **137**, 1111–1131, <https://doi.org/10.1175/2008MWR2638.1>.
- Zhang, R., A. Sumi, and M. Kimoto, 1996: Impact of El Niño the East Asian monsoon: A diagnostic study of the ‘86/87 and ‘91/92 events. *J. Meteor. Soc. Japan*, **74**, 49–62, https://doi.org/10.2151/jmsj1965.74.1_49.
- Zwiers, F., X. Zhang, and Y. Feng, 2011: Anthropogenic influence on long return period daily temperature extremes at regional scales. *J. Climate*, **24**, 881–892, <https://doi.org/10.1175/2010JCLI3908.1>.